IEEE Access
Multidisciplinary | Rapid Review | Open Access Journal

Received March 3, 2020, accepted March 26, 2020, date of publication March 31, 2020, date of current version April 16, 2020.

Digital Object Identifier 10.1109/ACCESS.2020.2984679

Hill-Start of Distributed Drive Electric Vehicle Based on Pneumatic Electronic Parking Brake System

LEI WU, HONGLIANG WANG, DAWEI PI, ERLIE WANG, AND XIA WANG
School of Mechanical Engineering, Nanjing University of Science and Technology, Nanjing 210094, China

Corresponding author: Hongliang Wang (whl343@163.com)

This work was supported in part by the Project of Jiangsu Provincial Six Talent Peaks under Grant 2016-JXQC-020, and in part by the Fundamental Research Funds for the Central Universities under Grant 309171B8811 and Grant 30919011265.

ABSTRACT The hill-start assist system (HAS) ensures that the vehicle starting on the ramp will not roll backwards, which improves the convenience of the driving in the case of starting on the ramp and parking. However, the traditional hill-start method is not suitable for distributed driving electric vehicles under some circumstances. Therefore, based on the pneumatic electronic parking brake system (EPB), a hill-start control method suitable for distributed driving electric vehicles is proposed in this paper, so as to realize the vehicle's fast and stable starting on the ramp. Firstly, by analyzing the change of the force of the vehicle during the starting of the ramp, a dynamic allocation strategy based on the front and rear axle loads is adopted in terms of demand torque. Secondly, according to the force analysis of the vehicle on the ramp, the control target of hill-start is determined, and the logic threshold control method is used to make the actual pressure change with the ideal pressure in real time. Then, a driving torque correction controller based on the sliding mode algorithm is designed to prevent driving wheels from slipping on bad roads, resulting in a reduction in the total driving force and a rollback of the vehicle. Finally, to verify its feasibility, Matlab, Trucksim and AMEsim were used to establish the controller model, the vehicle model and the pneumatic EPB system model for co-simulation verification. The simulation results show that the proposed control strategy can prevent the vehicle from slipping under different road conditions with less brake wear.

INDEX TERMS Distributed drive, hill start, sliding mode, coordinated control, moment correction, logical threshold, co-simulation.

I. INTRODUCTION

The hill start assist system is a technology that prevents the vehicle from rolling backwards when the vehicle starts uphill or downhill, and its control will directly affect the vehicle's dynamics and safety [1]. By merging or eliminating various unnecessary mechanical components, the hill start assist system is an advanced alternative to the traditional hand-brake system and can continue to provide braking force after the brake is released [2]. In addition, when the vehicle needs to start, the hill start assist system can judge when the driving force is greater than the motion resistance through the sensor, so as to release the braking force [3]. It makes the driver no longer need to complete the hill start by coordinating the clutch, handbrake and accelerator pedal, which greatly decreases the workload of the driver on the ramp. Therefore, the probability of driving accidents caused by operation errors is greatly reduced and unnecessary wear of brake components can be avoided. At present, the common parking brake systems of vehicles mainly include mechanical electronic brake systems, hydraulic electronic brake systems, and pneumatic electronic brake systems, etc [4]. However, the current hill-start assist system is mainly designed and applied to conventional gasoline-fueled automobiles. For distributed-driven vehicles, it has not been well adapted. Compared with traditional mechanical transmission vehicles, distributed drive electric vehicles eliminate complicated traditional systems such as transmissions and differentials. The drive motors of each wheel can be independently controlled, and single wheel driving/ braking torque control, inter-axis and inter-wheel

The associate editor coordinating the review of this manuscript and approving it for publication was Sudhakar Babu Thanikanti.

torque distribution control can be achieved accurately and quickly [5]–[7]. However, the distributed driving form of the vehicle places higher requirements on control strategy and algorithm of hill start [8].

In order to solve the control problem of hill start, researchers have proposed some solutions. A rapid control prototyping approach using design-based and RCP techniques was proposed to detect the drive-off condition of hill-start in real time and then an offset value is added to increase the low idle speed of engine [9]. A Hill Hold Mechanical concept that is both cost-saving and robust is proposed to prevent the vehicle from rolling back/forward when the vehicle starts in first or reverse gear, respectively. The controller processes CAN signals, such as clutch, accelerator, brake pedal positions, engine speed, vehicle speed, engine status, Hill Hold enable/disable switch, and battery status, and decides the number of rotations of the motor and thus the travel of the pin [10]. Researchers [11] proposed a new type of integrated feedforward-feedback compensation controller for the coordinated control of the clutch and Hydraulic Control Unit (HCU) of the Hill Start Assist Control (HAC) and the H1 control theory ensures stability and robustness.

For the traditional HAC strategy, the hill start controller will only release the parking brake force when it detects that the starting conditions of the vehicle on the ramp are satisfied, which will cause starting jitter and wear of brake. Researchers [12] proposed a hill start assist control strategy using bangbang control for commercial vehicles, so that the braking torque is gradually released as the driving torque increases. However, as the brake pressure increases, the period of the bangbang control will become longer, which will cause a relatively large delay in the release of braking force. Researchers [13]–[14] proposed a hill-start scheme based on logic threshold control to improve the accuracy of the HAC to some extent. However, if the above methods of the design for the traditional gasoline-fueled automobiles are directly applied to distributed drive electric vehicles, it may result in poor control or failure of the hill-start assist system. For example, the brakes are subject to a lot of wear or the vehicle is downhill for a long distance, etc.

In order to solve the problem of the hill start control of distributed driving electric vehicles, a new integrated control scheme is proposed to meet the requirements of the safety starting of the vehicle. First of all, according to the controllable characteristics of a single wheel of the distributed drive vehicle, a dynamic torque distribution strategy based on front and rear axle loads is adopted. Secondly, according to the force analysis of the hill start, a logic threshold control method with torque correction is designed to make the actual brake pressure change with the ideal brake pressure in real time. Finally, Matlab, Trucksim, and AMEsim were used to establish a co-simulation platform, and the effectiveness was verified in two road environments on a 20% slope. Evaluation indices, such as starting jerk, rollback distance and brake wear, are considered for comparison with the traditional control scheme.

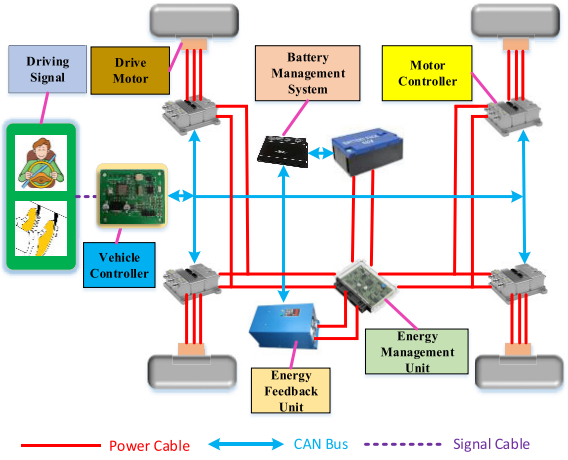

FIGURE 1. Block diagram of distributed driving electric vehicle.

II. SYSTEM MODELS

A. VEHICLE MODEL

When the vehicle starts on the hill, under the influence of the component force of the vehicle weight along the downward direction of the hill, the vehicle will have a tendency to slide down the slope. Therefore, it is necessary to coordinate the control of the clutch and the braking system, and complete the hill start of the vehicle through the reasonable coordination of the braking torque and the torque transferred by the clutch.

The structural block diagram of the distributed drive electric vehicle is shown in Fig. 1. It mainly includes a power supply system, a drive motor system, and a vehicle controller system. The vehicle controller analyzes the acceleration / brake pedal signals and steering wheel angle signals from the driver, monitors the vehicle's driving status, coordinates the control unit, makes the corresponding judgments, and then sends the target instructions to each drive motors of the lower lever through the CAN bus. It also cooperates with the battery management system for functions such as energy recovery and fault diagnosis. The drive motor system mainly includes each motor controller and each drive motor. As one of the key parts of an electric vehicle, the motor controller converts the electric energy stored in the power battery into the electric energy required to start the motor according to the instructions of gear, acceleration and brake, etc. to control the motor's speed, torque, rotation direction, response time and other motion states [15]. The power supply system mainly includes power battery, battery management system and so on. The battery management system is a set of control systems to protect the safety of the power battery. It monitors the use of the power battery in real time, controls the charge and discharge of the battery, and estimates the battery status to send signals of display and alarm to the on-board information display system through the CAN bus, ensuring the safety of the vehicle. The basic parameters of the distributed drive electric vehicle studied in this paper are shown in Table 1.

TABLE 1. Basic parameters of distributed driving electric vehicles.

Variables	Notation	Value	Unit
Vehicle mass	M	5320	kg
Moment of inertia around the Z axis	I_z	31365	kg·m^2
Distance from the front axle to the mass center	a	3	m
Wheelbase	L	5	m
Centroid height	H	1.175	m
Wheel effective radius	R_w	0.487	m

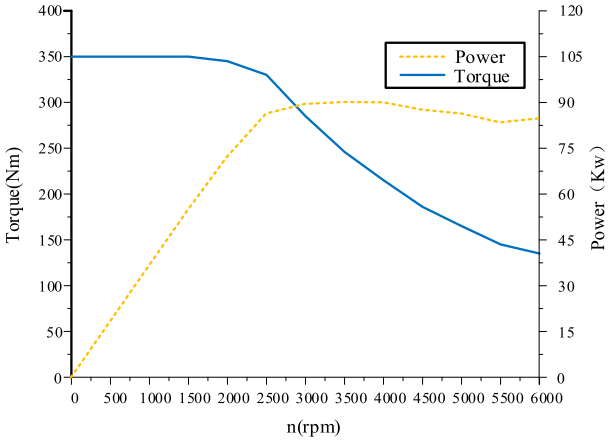

FIGURE 2. The external characteristic curve of the motor.

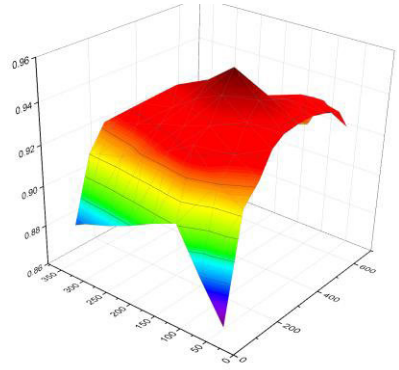

FIGURE 3. Motor efficiency map.

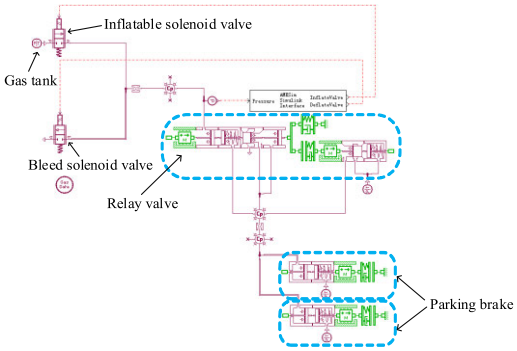

FIGURE 4. Model of the pneumatic EPB system.

B. DRIVE MOTOR MODEL

The drive motor is the core component of the entire electric drive system, especially for electric drive vehicles that use a series hub motor drive solution. All the power of the entire vehicle is ultimately transmitted to the drive wheels by the drive motor, so the performance of the drive motor directly determines the maneuverability of the vehicle.

The drive motor is usually required to be able to start/stop, accelerate/decelerate frequently. Large torque is required for low speed and small torque is required for high speed driving during the hill start [16]. Its main parameters include: motor type, rated voltage, mechanical characteristics, efficiency, dimensional parameters, reliability and cost. In order to meet the vehicle's maximum climbing capability of 35% and maximum speed of 135 km/h, a permanent magnet synchronous motor with peak torque of 350 Nm and peak power of 90 kw was selected. The external characteristic curve is obtained by fitting the experimental data of the permanent magnet synchronous motor (PMSM), as shown in Fig. 2. The efficiency of the motor can be simplified as a function of the motor speed and the demand torque. The motor efficiency map is shown in Fig. 3.

The torque model of the motor can be simplified into a first-order dynamic system model of formula (1):

$$\dot{T_{act}} = \tau \left(\eta T_{ref} - T_{act}\right) \tag{1}$$

where, η is the efficiency of the motor, T_{ref} is the expected output torque of the motor. The motor's ideal characteristic curve method is used to establish a motor model to make the torque response of the motor equivalent to the response of the motor current. The current response time is milliseconds and the motor time constant τ describes the speed of the motor response. The value of τ is 0.1.

C. EPB MODEL

The components of the pneumatic EPB system are shown in Fig. 4. It mainly includes solenoid valves, relay valves, parking brake chambers, a gas storage tank, many connected gas pipelines, and various sensors. The EPB system replaces the parking manual control valve with an electronic switch. The charge and bleed solenoid valves are on-off valves. At the same time, to improve the control effect of the EPB system, an air pressure sensor and an acceleration sensor are installed in the system. The air pressure sensor installed at the control port of the relay valve measures the air pressure in the brake chamber by directly measuring the air pressure at the control port [17]. The acceleration sensor is embedded in the EPB controller to measure the road slope and the longitudinal acceleration of the vehicle. To add or release the parking brake force, the EPB controller receiving signals from electronic switches, CAN bus, air pressure sensor and acceleration sensor controls the motions of the charge and bleed solenoid valve according to internal control algorithms.

When the vehicle starts on a slope, the driver presses the parking brake switch button, and the switch signal is sent to the ECU. The EPB system checks whether all conditions are

met. Once the conditions for parking brake release are met, the parking brake system automatically releases the parking brake force. At this time, the ECU activates the solenoid valve to act so that the compressed air from the air compressor enters the control port on the relay valve, then opens the output port on the relay valve. Then the compressed air at the supply port of the parking brake can be released. When the parking brake needs to be released, the driver pushes the switch button, and the EPB controller controls the charge solenoid valves to open so that the high-pressure gas in the gas storage tank enters the control port of the relay valve. Then, the inlet and outlet of the relay valve are connected, the high-pressure gas in the gas storage tank enters the parking brake air chamber to release the parking brake; when the parking brake needs to be applied, the ECU controls the bleed solenoid valves to open. Any air between the relay control port and the solenoid valve is discharged through the bleed solenoid valves. After that, the air supply between the air inlet and outlet of the relay valve is cut off, and the high-pressure air in the parking brake chambers is exhausted through the exhaust port of the relay valve.

Because the solenoid valve is the main component of the EPB system, its dynamic characteristic has great influence on the EPB system. When the HSA system is working, the solenoid valve of the EPB system can be considered as an on / off valve, and the pressure of the parking brake chamber is adjusted by opening / closing the solenoid valve. The dynamic characteristics of the solenoid valves include circuit model, magnetic circuit model and dynamic model of mechanical components [18].

The electromagnetic model of the solenoid valve is expressed as follows:

$$\begin{cases} U = IR + N\dfrac{d\emptyset}{dt} \\ IN = \dfrac{\sigma\emptyset}{\mu A_c} \end{cases} \tag{2}$$

where, I is the working current of the coil (A);U is the working voltage of the solenoid valve (V); R is the internal resistance of the coil (Ω); $\emptyset$ is the magnetic flux of the coil; t is the time; N is the total turns of the coil.

The dynamic model of the mechanical component can be shown as follows:

$$\ddot{x} = \frac{1}{m_e}\left[\frac{\emptyset^2}{2\mu_e A_c} - P_e A_e - K_e\left(x + x_p\right) - c\dot{x}\right] \tag{3}$$

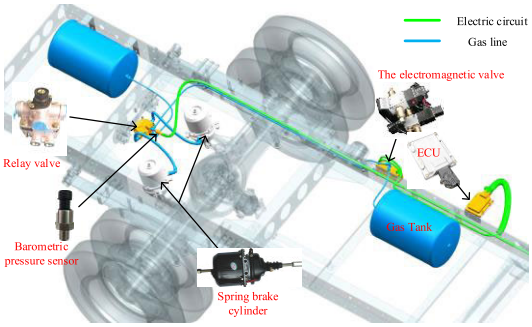

FIGURE 5. The structure diagram of the EPB system.

where, m_e is the mass of valve core; x is the movement distance of valve core; c is the equivalent viscous damping of valve core movement; K_e is the return spring stiffness of solenoid valve; P_e is the air pressure of control port; x_p is the return spring preload; A_e is the cross-sectional area of valve core; A_c is the cross-sectional area at the air gap; μ_e is the air permeability.

Ignoring heat transfer, the dynamic equation of the parking brake chamber is as follows, (4) as shown at the bottom of this page, where, C_k is the flow coefficient; C_s is the flow coefficient of valve hole; T is the temperature of the gas; R_{gs} is the ideal gas constant; γ is the adiabatic index. During inflation, P_{us} is a fixed value. P_{ds} is the pressure of the brake chamber.

The pneumatic EPB system model is shown in Fig. 5. Table 2 lists the main parameters of the system.

III. CONTROL SYSTEM DESIGN

For the hill start controller proposed in this study, signals such as vehicle speed, road slope, accelerator and brake pedal are collected for processing and determining whether the braking system needs to be activated. Once it is determined through analysis that the vehicle is going to start on a ramp, the brake force will be released in time. In this paper, based on the pneumatic electronic parking brake system, a hill-start control method suitable for the distributed driving electric vehicle on the ramp is proposed to achieve fast and stable starting.

A. OVERALL ARCHITECTURE OF VEHICLE CONTROLLER

The actual motion state of the vehicle is the result of cooperation of many components, and the controller is the core of

$$\frac{dP}{dt} = \begin{cases} 0.0405 C_k C_s x \dfrac{P_{us}}{\sqrt{T}} & \dfrac{P_{us}}{P_{ds}} < 0.528 \\ C_k C_s x \dfrac{P_{us}}{\sqrt{T}} \left(\dfrac{2\gamma}{R_{gs}(\gamma - 1)} \left(\left(\dfrac{P_{us}}{P_{ds}}\right)^{\frac{2}{\gamma}} - \left(\dfrac{P_{us}}{P_{ds}}\right)^{\frac{\gamma+1}{\gamma}} \right) \right)^{\frac{1}{2}} & \dfrac{P_{us}}{P_{ds}} \geq 0.528 \end{cases} \tag{4}$$

TABLE 2. Main parameters of pneumatic EPB system.

Parameter	Unit	Value	Parameter	Unit	Value
Voltage	V	24DC	Relay valve piston diameter	mm	80
Coil resistance	Ω	41	Relay valve diameter	mm	24
Air gap cross-sectional area	m^2	4.72×10^{-5}	Stiffness of piston return spring	N/mm	0.77
Spool quality	kg	0.02	Valve return spring stiffness	N/mm	5.39
Solenoid valve hole diameter	mm	2.2	Preload of piston return spring	N	10
Coil turns	-	600	Valve return spring preload force	N	140
Air gap length	m	0.001	Brake chamber piston diameter	mm	120
Spool cross-sectional area	m^2	5.03×10^{-5}	Brake chamber piston rod diameter	mm	25
Relay valve piston mass	kg	0.033	Brake chamber volume	m^3	0.00265

these components. By analyzing the vehicle driving signals and combining the state feedback information of the vehicle, the controller executes the corresponding control algorithm commands inside the controller, and finally sends the control signals to the actuators to correct the vehicle's motion state. The actuators in this paper mainly include four driving motors and two pneumatic EPB parking brake systems mounted on the rear axle. According to the torque commands issued by the motor controllers and the current running state of the motors, the four driving motors output the actual driving torque acting on the wheels to realize the driving intention.

As shown in Fig. 6, the distributed drive electric vehicle hill start controller proposed in this paper is mainly divided into three layers, namely the driving torque pre-distribution controller in the upper layer, the torque correction controller in the middle layer and the parking control controller in the bottom layer.

The hill-start controller flowchart in Fig. 7 shows the process of control. First, according to the identified driving intention of the driver mainly including the accelerator pedal

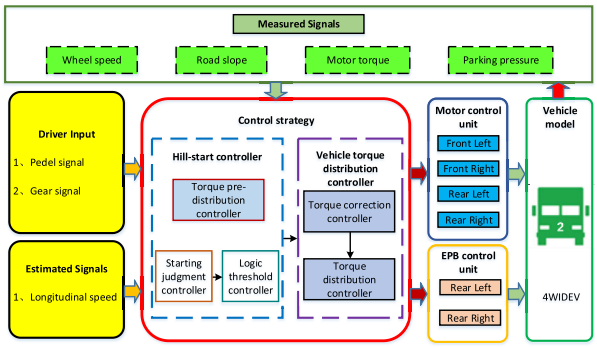

FIGURE 6. The overall structure of the controller.

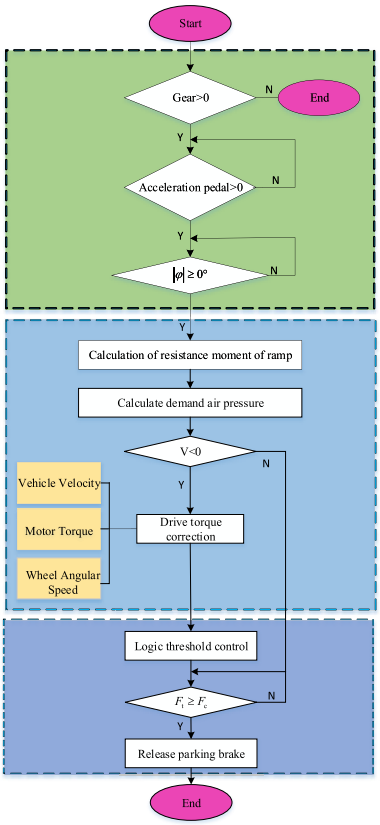

FIGURE 7. Flow chart of the hill start controller.

signal and the gear signal, the driving torque pre-distribution controller in the upper layer obtains the reference total torque of the drive motor, and then predistributes the motor torque of the front and rear axle. Due to the uneven distribution of mass, the vehicle's center of mass is not at the geometric center. In other words, the adhesion capacity of the front and rear axles on the same adhesion coefficient road surface will be affected by the driving state of the vehicle. Therefore, the torque predistribution method based on the front and rear axle loads is used in this paper.

Secondly, during the process of starting on a ramp, the vehicle is prone to slip on low-adhesion road or undulating road, which affects the effect of the hill start. In severe cases, it will even slip down the ramp, leading to the failure of

the hill start and irreparable loss of the driver's life and property [19]–[21]. Therefore, in the middle torque correction layer, anti-slip control is the core. When the wheel coverslips, the torque correction controller can calculate the desired torque of each drive motor. By using the sliding mode control method to detect the speed and direction of the wheel, the demand torque of the drive motor can be adjusted in real time to prevent the vehicle from losing stability on the ramp. In addition to controlling the driving torque of the slipping wheels, the torque distribution controller will redistribute the driving torque reasonably and quickly according to the modified torque. The motor control unit coordinates the actual output torque of each motor by receiving the desired torque signal of each motor to realize the vehicle's safety.

Finally, the start judgment controller determines whether the starting conditions meet the requirements to trigger the vehicle's hill start controller. The logic threshold controller calculates the demand pressure of the parking brake in real time and controls the air pressure of the parking brake air chamber according to the logic threshold control method to make it follow the change of the demand pressure. In this process, each wheel speed and vehicle speed are monitored in real time. When the monitored acceleration is less than 0, it is indicated that the vehicle has a roll backwards trend, and the demand pressure is recalculated immediately according to the corrected torque of the middle torque correction layer. Then the hill start control system continues to release the parking brake force according to the logic threshold control method. When the driving torque is greater than the resistance, the inflation solenoid valve is often opened until the parking brake is removed. The EPB control unit receives the demand pressure command sent by the logic threshold controller and controls the EPB actuator to gradually release the brake force to complete the hill start control.

B. DESIGN OF HILL START CONTROLLER

1) VEHICLE DYNAMICS ANALYSIS

As shown in Fig. 8, when the vehicle starts on the ramp, the force of gravity generates a downward resistance to the vehicle along the ramp, and the vehicle has a downward movement tendency. By controlling the throttle and gear, the driver makes the motor generate the driving force along the ramp upward. Before the driving force overcomes the resistance, the direction of the braking force goes up along the slope to help the driving force maintain the vehicle's static state and prevent the vehicle from rolling back [22].

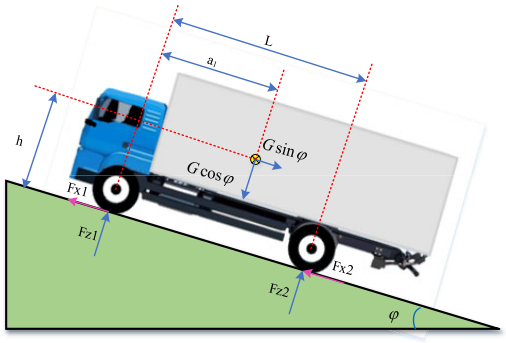

FIGURE 8. Force analysis of the vehicle on the ramp.

The following equation can be obtained by using the force and moment balance equation:

$$\begin{cases} F_{x1} + F_{x2} - \dfrac{1}{2} C_d \rho_a S V^2 + Mg\,(sin\varphi + \mu_a cos\varphi) = Ma \\ F_{z1} + F_{z2} - Mgcos\varphi = 0 \\ -F_{z1} a_1 + F_{z2}\,(L - a_1) - (F_{x1} + F_{x2}) \cdot h = 0 \end{cases} \tag{5}$$

By eliminating F_{x1} and F_{x2}, the normal force F_{z1} and F_{z2} based on vehicle dynamics can be obtained, (6) as shown at the bottom of this page.

Therefore, the demand torque of each driving motor is:

$$T_{refi} = \frac{F_{zi}}{2\sum_{i=1}^{2} F_{zi}} T_{tot} \tag{7}$$

where $M, g, R_\omega, \varphi, V, C_d, \rho_a, S$ represent the total mass of the vehicle, the acceleration of gravity, the effective radius of the wheel, the road slope, the vehicle speed, the air drag coefficient, the air density, and the effective windward area respectively; F_{x1} and F_{x2} respectively represent the road driving force of the front and rear axles of the vehicle; F_{z1} and F_{z2} refer to the normal forces on the front and rear axles respectively; T_{tot} is the total moment required at the moment; μ_a is the rolling friction coefficient of the tire; h is the height of the centroid; a_1 and L are refer to the distance from the center of mass to the front axis and the wheelbase respectively; a is the acceleration of the vehicle.

The longitudinal dynamic equation of the vehicle [23]

$$\begin{cases} \dfrac{\sum_{i=1}^{4} T_{acti} + T_{brk} - \sum_{i=1}^{4} T_{di}}{R_\omega} \\ \quad = \dfrac{1}{2} c_d \rho_a S V^2 + Mg\,(sin\varphi + \mu_a cos\varphi) \\ M\dot{V} = \dfrac{\sum_{i=1}^{4} T_{di}}{R_\omega} \end{cases} \tag{8}$$

$$\begin{cases} F_{z1} = \dfrac{M \cdot g \cdot cos\varphi\,(L - a_1 - \mu_a h) - M \cdot g \cdot sin\varphi \cdot h - Ma - \dfrac{1}{2} C_d \rho_a S V^2}{L} \\ F_{z2} = \dfrac{M \cdot g \cdot sin\varphi \cdot h + M \cdot g \cdot cos\varphi\,(a_1 + \mu_a h) + \dfrac{1}{2} C_d \rho_a S V^2 + Ma}{L} \end{cases} \tag{6}$$

where, $\sum_{i=1}^{4} T_{di}$ and $\sum_{i=1}^{4} T_{acti}$ are the final effective driving torque of the vehicle and the driving torque acting on the wheels; T_{brk} is the braking torque of a single wheel generated by the static friction of the tire and the pneumatic brake system and meets:

$$\begin{cases} T_{brk} = min\{\mu_0 MgR_\omega cos\varphi, \epsilon P_{act}\} \\ P_{act} \le P_{max} \end{cases} \tag{9}$$

where, μ_0 is the static friction coefficient of the tire; ϵ, P_{act} and P_{max} are the pressure conversion coefficient, the actual and maximum braking pressure of the pneumatic parking brake system.

During the entire starting process, the vehicle speed V is generally small (ideally, it is always 0), so the air resistance is less than the rolling resistance and ramp resistance of the vehicle. So, the nonlinear term of (8) can be linearized to $\frac{1}{2}c_d\rho_a SV^2 \approx c_d\rho_a SV$ based on the first-order Taylor linearization. Define the state variable of the system state equation as $x = \begin{bmatrix} T_{act1} & T_{act2} & T_{act3} & T_{act4} & V \end{bmatrix}^T$; The input variable is $u = \begin{bmatrix} T_{t1} & T_{t2} & T_{t3} & T_{t4} & T_{brk} \end{bmatrix}^T$ and the output variable of the system is y = x.

According to equations (5)-(8), the system model is:

$$\begin{cases} \dot{x} = Ax + Bu + \varpi \\ y = Cx + D\varpi \end{cases} \tag{10}$$

where,

$$A = \begin{bmatrix} -\tau & 0 & 0 & 0 & 0 \\ 0 & -\tau & 0 & 0 & 0 \\ 0 & 0 & -\tau & 0 & 0 \\ 0 & 0 & 0 & -\tau & 0 \\ \frac{1}{MR_\omega} & \frac{1}{MR_\omega} & \frac{1}{MR_\omega} & \frac{1}{MR_\omega} & -\frac{C_d\rho_a S}{M} \end{bmatrix};$$

$$B = \begin{bmatrix} \tau\eta & 0 & 0 & 0 & 0 \\ 0 & \tau\eta & 0 & 0 & 0 \\ 0 & 0 & \tau\eta & 0 & 0 \\ 0 & 0 & 0 & \tau\eta & 0 \\ 0 & 0 & 0 & 0 & \frac{2}{MR_\omega} \end{bmatrix};$$

$$C = \begin{bmatrix} 1 & 0 & 0 & 0 & 0 \\ 0 & 1 & 0 & 0 & 0 \\ 0 & 0 & 1 & 0 & 0 \\ 0 & 0 & 0 & 1 & 0 \\ 0 & 0 & 0 & 0 & 1 \end{bmatrix};$$

$$D = \begin{bmatrix} 0 & 0 & 0 & 0 & 0 \end{bmatrix};$$

$$\varpi = \begin{bmatrix} 0 & 0 & 0 & 0 & -g(sin\varphi + \mu_a cos\varphi) \end{bmatrix}^T$$

2) SPEED ESTIMATION

The estimation accuracy of the longitudinal speed directly determines the control effect of the driving torque correction module in this paper. Therefore, the vehicle speed information needs to be obtained accurately and in real time. At present, there are two main methods for obtaining the longitudinal speed of the distributed driving vehicle: one is to use an optical sensor or a high-precision GPS speedometer; the other is an estimation method based on common on-board sensors [24]. The former method is not suitable for large-scale production and general research because the cost is too high, so the second method has become the mainstream of current research. In this paper, the Kalman filter method is used to estimate the driving state parameters of the car. The wheel speed signals of the four wheels are selected as the observed quantity, and an acceleration sensor is installed at the center of mass of the vehicle to obtain the acceleration information of the vehicle.

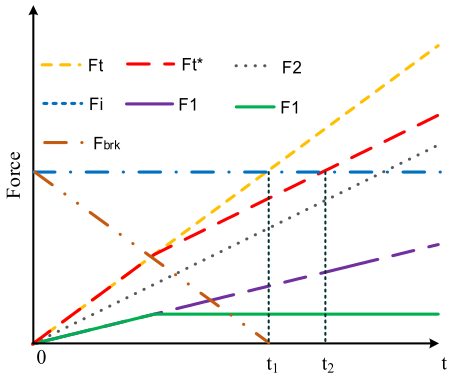

FIGURE 9. Schematic diagram of the starting process of the ramp.

The speed estimation recursive equation based on kalman filter was obtained as follows:

$$\begin{cases} W^-(k) = W(k-1) + Q \\ K(k) = P^-(k)H^T\left[\left(HW^-(k)\right)H^T + R(k)\right]^{-1} \\ \hat{v}(k+1) = v(k) + \sigma a(k) \\ \hat{\omega}(k+1) = H\hat{v}(k+1) \\ v(k+1) = \hat{v}(k+1) + K(k+1) \\ \qquad \left(\omega(k+1) - \hat{\omega}(k+1)\right) \\ P(k) = (I - K(k)H)P^-(k) \end{cases} \tag{11}$$

where, $W(k)$ is the error covariance matrix; $a(k)$ is the acceleration at time $t(k)$; $R(k)$ is the variance of the measurement noise Q; $v(k)$ and $\hat{v}(k+1)$ are the estimated value and the prior estimate value of the vehicle speed at time $t(k+1)$; $\omega(k+1)$ and $\hat{\omega}(k+1)$ are the measured value and the predictive value of wheel speed at time $t(k+1)$; $K(k)$ is the Kalman filter gain matrix at time $t(k)$ and its expression is: $K = \begin{bmatrix} k_{fl} & k_{fr} & k_{rl} & k_{rr} \end{bmatrix}$. $k_i, i = fl, fr, rl, rr$ represent the gain values of the left front wheel, left rear wheel, right front wheel, and right rear wheel respectively.

When a wheel is slipping, the parameter in the gain matrix is adjusted so that the element value corresponding to the wheel is reset to zero. If the wheels do not slip, the element values obtained from the recursive formula of the Kalman filter are used to calculate, so as to obtain a more accurate vehicle speed estimate.

3) ANALYSIS OF HILL START

A schematic diagram of the hill-start process is shown in Fig. 9. As can be seen from the figure, when the vehicle starts on the ramp, the parking braking force F_{brk} provided

by the EPB system gradually decreases as the total driving force F_t of the vehicle increases. At time t_1, the total driving force of the vehicle $F_t = F_{x1} + F_{x2}$, which is exactly equal to the slope resistance F_ξ. In an ideal state, when the driving force just overcomes the slope resistance, it should be ensured that the parking brake force is completely removed at this moment. However, when distributed drive vehicle starts on the ramp in reality, some wheels (assuming one or two wheels on the front axle) may slip due to the uneven road surface or too low road adhesion coefficient. In this case, the actual total driving force of the vehicle $F_t^* = F_{x1}^* + F_{x2}$ is less than the nominal total driving force of the vehicle F_t, that is $F_t^* < F_t$. If the parking brake at this time gradually releases the parking brake force according to the nominal total vehicle driving force F_t, it will cause the vehicle parking brake to release the braking force in advance, resulting in the braking force and driving force being insufficient to maintain the vehicle's stationary state. In this case, if not controlled, the vehicle will run in the risk. Therefore, in order to improve the control effect of the hill start and avoid the vehicle rolling backwards, the driving force of the vehicle needs to be modified, and then the parking control unit gradually releases the braking force as the modified total driving force increases, so that the parking brake force is completely released at time t_2.

To facilitate the study, the braking force of EPB F_{brk} is simplified as:

$$F_{brk} = F_{bmax} - \frac{F_{bmax}}{P_{max}} P_{act} \tag{12}$$

In the formula, F_{bmax} is the maximum parking braking force, N; P_{max} is the pressure when the parking brake force is completely released, MPa.

According to the analysis in Fig. 9, the control goal of hill start is to make the braking force F_{brk} follow the curve in the figure, namely:

$$F_{brk} = F_\xi - \sum_{i=1}^{4} F_{ti} \tag{13}$$

where, the driving force and slope resistance can be calculated according to equations (14) and (15):

$$\sum_{i=1}^{4} F_{ti} = \frac{\sum_{i=1}^{4} T_{acti}}{R_\omega} \tag{14}$$

$$F_\xi = C_d \rho_a S V + Mg(sin\varphi + \mu_a cos\varphi) \tag{15}$$

Combining formula (5), (8), (12), and (14), it can be obtained that the demand pressure P_{dem} during the hill start control process is:

$$P_{dem} = \left(F_{bmax} + \frac{\sum_{i=1}^{4} T_{ti}}{R_\omega} - C_d \rho_a S V - Mg(sin\varphi + \mu_a cos\varphi) \right) \times \frac{P_{max}}{F_{bmax}} \tag{16}$$

It can be seen that the goal of the hill start control proposed in this paper is to control the pressure of the parking brake P_{act} and make it follow the change of the demand pressure P_{dem} calculated by formula (16).

For the distributed drive electric vehicle, each wheel is independently controlled by a motor, and the total driving force of the vehicle is the sum of the driving motor's driving forces. if some wheels slip during the hill start, the calculation of the demand pressure would be greatly deviated, resulting in the release in advance of the EPB before the slope resistance has been completely overcome by the driving force. It will lead to the failure of the hill start. By analyzing the effect of the hill start control on the ramp when the actual driving torque of the vehicle control system is less than the theoretical driving torque, a method for correcting the driving torque during the starting on the ramp is proposed.

The motion equation of each wheel is as follows

$$\begin{cases} I_\omega \dot{\omega_{fl}} = i_m T_{tfl} - R_\omega F_{xfl} \\ I_\omega \dot{\omega_{fr}} = i_m T_{tfr} - R_\omega F_{xfr} \\ I_\omega \dot{\omega_{rl}} = i_m T_{trl} + \mathrm{T_b} - R_\omega F_{xrl} \\ I_\omega \dot{\omega_{rr}} = i_m T_{trr} + \mathrm{T_b} - R_\omega F_{xrr} \end{cases} \tag{17}$$

where, I_ω is the moment of inertia of the wheel.

The linear sliding surfaces are selected as follow:

$$\begin{cases} S_1 = \omega_{fl} - \omega_{fld} \\ S_2 = \omega_{fr} - \omega_{frd} \\ S_3 = \omega_{rl} - \omega_{rld} \\ S_4 = \omega_{rr} - \omega_{rrd} \end{cases} \tag{18}$$

where, $\omega_{id}, i = fl, fr, rl, rr$ are the desired values of the wheel speeds corresponding to the four wheels.

The index approach laws are shown below:

$$\begin{cases} \dot{S_1} = -k_1 S_1 - \varepsilon_1 sgn(S_1) \\ \dot{S_2} = -k_2 S_2 - \varepsilon_2 sgn(S_2) \\ \dot{S_3} = -k_3 S_3 - \varepsilon_3 sgn(S_3) \\ \dot{S_4} = -k_4 S_4 - \varepsilon_4 sgn(S_4) \end{cases} \tag{19}$$

where, $\varepsilon_i > 0, i = 1, 2, 3, 4$ determine the approaching speed. The larger the value, the faster the approaching speed will be, but it may cause a relatively large chatter after reaching the sliding mode surface. By adjusting the values of $k_i > 0, i = 1, 2, 3, 4$, the non-sliding mode motion can be effectively guaranteed to have good quality.

$$\begin{cases} \dot{S_1} = \dot{\omega_{fl}} - \dot{\omega_{fld}} \\ \dot{S_2} = \dot{\omega_{fr}} - \dot{\omega_{frd}} \\ \dot{S_3} = \dot{\omega_{rl}} - \dot{\omega_{rld}} \\ \dot{S_4} = \dot{\omega_{rr}} - \dot{\omega_{rrd}} \end{cases} \tag{20}$$

By eliminating variables, the torque correction value of each driving wheel can be obtained, as (21) shown at the bottom of the next page:

4) HILL START CONTROLLER

From the above analysis, it can be known that the control goal of the hill start controller is to make the actual pressure of the parking brake chamber effectively and timely follow the change of the demand pressure calculated by formula (16).The pressure of the parking brake chamber can be adjusted by the opening and closing of the EPB solenoid valve, so the key point of the hill start control

method proposed in this paper is to choose the appropriate control method of the solenoid valve to control the action of the solenoid valve.Therefore, a fast response control strategy of the solenoid valve based on logic threshold control is proposed. Because the logic threshold control method only needs to set reasonable threshold values according to the system characteristics, instead of establishing complex control model. Once the threshold is set reasonably, it will obtain satisfactory control performance. It is especially suitable for nonlinear systems such as the hill start assist system based on EPB. The control method is widely used in engineering control and has been proved to be very practical.

According to the pressure characteristics of the pneumatic EPB system, the system will have different delay times under different solenoid valve opening time. A large number of experiments show that the delay time of the EPB system used in this paper is maintained at about 40 milliseconds, so 40 milliseconds is selected in this paper as the shutdown time in a control cycle. The pulse width frequency modulation (PWM-PFM) method is adopted to control the on / off of the solenoid valve, and the inflation rate and the pressure change value of the pneumatic EPB system are changed by adjusting the duty cycle and frequency of the control signal. As shown in Figure 10, The two threshold values are e_1 and e_2 respectively. In combination with the pressure change characteristics of the pneumatic EPB system, e_1 is set as 0.05 MPa and e_2 is set as 0.1 MPa. The logic threshold control method judges the threshold range of the pressure difference P_{err} between the actual air pressure P_{act} and the required air pressure P_{dem} of the parking brake chamber, and adjusts the solenoid valve by sending the corresponding PWM control signals to the solenoid valve to control the rate of inflation or deflation,making the actual pressure of the parking brake chamber change with the demand pressure. When $P_{err} \geq P_{dem} - e_2$ or $-P_{err} \geq P_{dem} + e_1$, the large duty cycle control signals are used to control the charge and bleed solenoid valves to reduce the pressure difference quickly; when $P_{err} \geq P_{dem} - e_1$ or $-P_{err} \geq 0$, the small duty cycle control signals are used to control the charging and deflation solenoid valve actions to accurately follow the required air pressure; when $0 < P_{err} < P_{dem} - e_1$, the current state is maintained so that the actual pressure in the parking brake chamber is always lower than the demand pressure to prevent the vehicle from rolling backwards caused by overcharging.

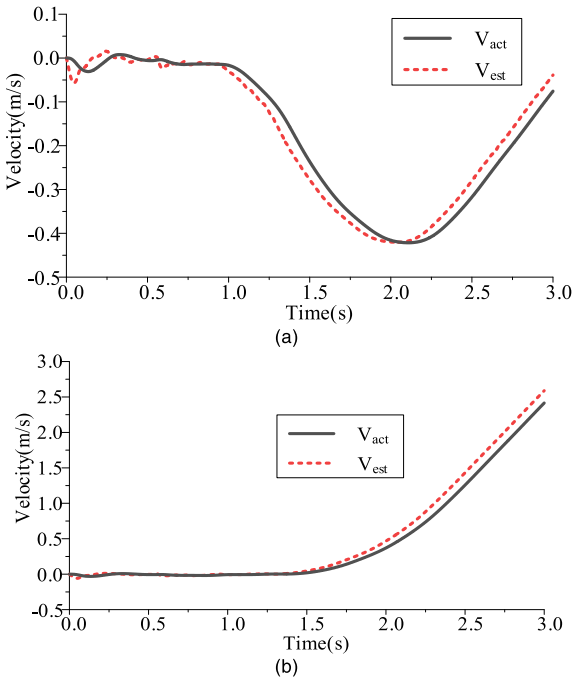

FIGURE 10. Velocity estimation under two conditions. (a) Bad road conditions, (b) Good road conditions.

TABLE 3. Statistics of vehicle speed estimation errors.

Test	Maximum error value	Unit
Bad road	0.053	m/s
Good road	0.176	m/s

IV. EVALUATION INDEX

A. RIDING COMFORT

In order to improve the ride comfort when starting on a hill and avoid large impacts during starting, the final driving torque T_{tot} should be gradually increased. The starting jerk J uses the change rate of the longitudinal acceleration of the vehicle as shown in formula (22) as a performance index of

$$\begin{cases} T_{t1} = \dfrac{\left(\rho\dot{\omega_{fl}} - k_1 S_1 - \varepsilon_1 sgn\left(S_1\right) + \dot{\omega_{fld}}\right) I_\omega] + R_\omega \left(\dot{F_{xfl}} + \rho F_{xfl}\right)}{i_m \rho} \\ T_{t2} = \dfrac{\left(\rho\dot{\omega_{fr}} - k_2 S_2 - \varepsilon_2 sgn\left(S_2\right) + \dot{\omega_{frd}}\right) I_\omega] + R_\omega \left(\dot{F_{xfr}} + \rho F_{xfr}\right)}{i_m \rho} \\ T_{t3} = \dfrac{\left(\rho\dot{\omega_{rl}} - k_3 S_3 - \varepsilon_3 sgn\left(S_3\right) + \dot{\omega_{rld}}\right) I_\omega] - \mathrm{T_b} + R_\omega \left(\dot{F_{xrl}} + \rho F_{xrl}\right)}{i_m \rho} \\ T_{t4} = \dfrac{\left(\rho\dot{\omega_{rr}} - k_4 S_4 - \varepsilon_4 sgn\left(S_4\right) + \dot{\omega_{rrd}}\right) I_\omega] - \mathrm{T_b} + R_\omega \left(\dot{F_{xrr}} + \rho F_{xrr}\right)}{i_m \rho} \end{cases} \tag{21}$$

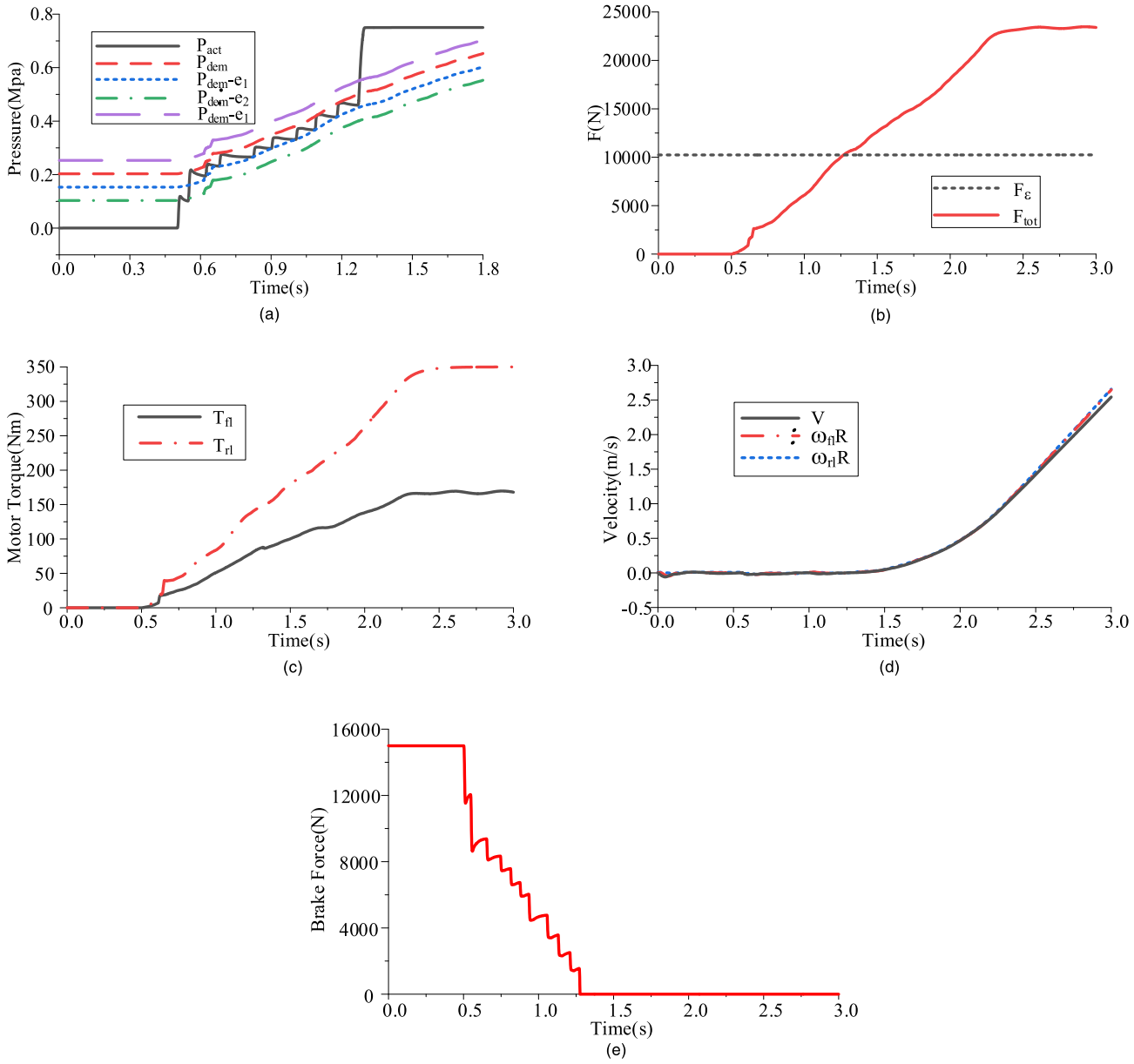

FIGURE 11. Simulation results of the equal torque distribution strategy. (a) Pressure, (b) Force, (c) Motor torque, (d) Vehicle speed and wheel speed, (e) Brake force.

riding comfort.

$$J = \frac{da}{dt} \tag{22}$$

B. GETTING STARTED SAFETY

During the process of starting a vehicle on a slope, if the vehicle slides too far, it will easily cause a traffic accident and cause serious consequences to the driver's life and property. Therefore, the vehicle cannot roll down or the slope distance L should be less than a certain threshold during the entire hill-start process and the expected speed V should satisfy $V = 0$.

$$L = \int_0^t Vdt \geq 0 \tag{23}$$

C. BRAKE WEAR

Improper control during the start of the ramp will cause excessive wear of the parking brake, and in severe cases may directly lead to a complete failure. To reduce the wear of the braking system during the entire process, the following performance indicators should be adopted:

$$\begin{cases} \int_0^t \dfrac{|2T_b|\,V}{R} dt \\ T_b \geq 0 \end{cases} \tag{24}$$

The former formula of the formula (24) represents the friction work of the parking brake system, and the latter formula is a condition to avoid the parking brake force becoming the resistance of the hill-start.

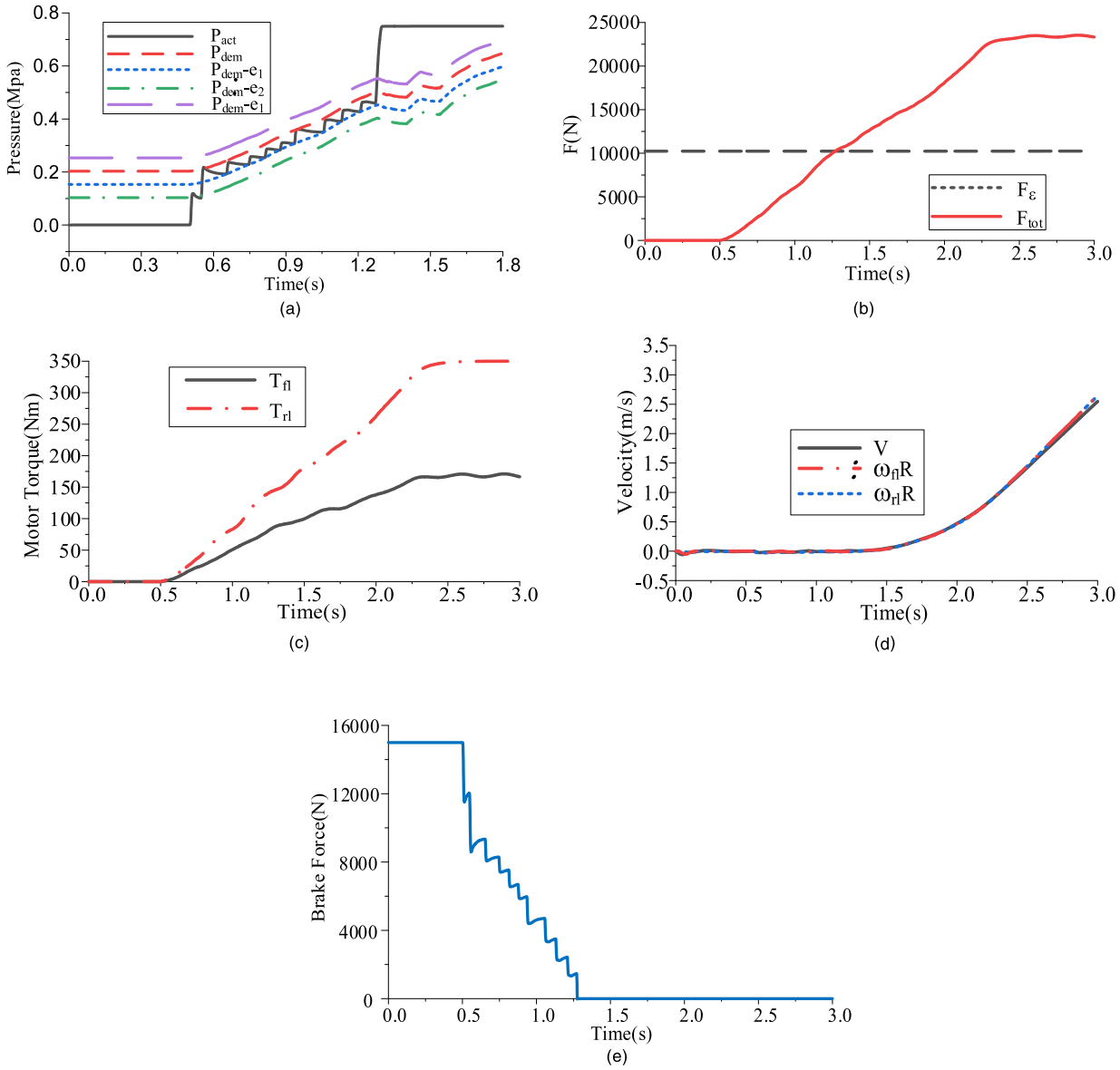

FIGURE 12. Simulation results of dynamic torque distribution strategy. (a) Pressure, (b) Force, (c) Motor torque, (d) Vehicle speed and wheel speed, (e) Brake force.

V. SIMULATION AND ANALYSIS

In this section, to evaluate the performance of the designed hill-start controller, Matlab, Trucksim and AMEsim are used for co-simulation verification. In Matlab / Simulink, the hill-start controller model and the driving motor model are established, the distributed driving vehicle model is established in Trucksim by modifying structure parameters, and the pneumatic EPB system model is established in AMEsim software. The simulation was performed on a 20% slope, and the test was evaluated by comparing the two road adhesion conditions with the method of 'expected driving torque evenly distributed' and 'no torque correction'. It is important to point out that to prevent unexplained interference before the simulation, all the control strategies in this paper start to work after 0.5s, before which the vehicle is stationary on the slope.

A. VERIFICATION OF VEHICLE SPEED ESTIMATION

The speed estimation ability determines the control effect of the torque correction controller. In this paper, the effect of the vehicle speed estimation will be simulated and evaluated under the condition of good road surface and ice and snow road surface. Fig. 10 shows the effect of vehicle speed estimation under two conditions, where *V_act* represents the actual value of the longitudinal speed of the vehicle; *V_est* represents the estimated value of the longitudinal speed. Table 3 reveals the statistics of vehicle speed estimation errors.

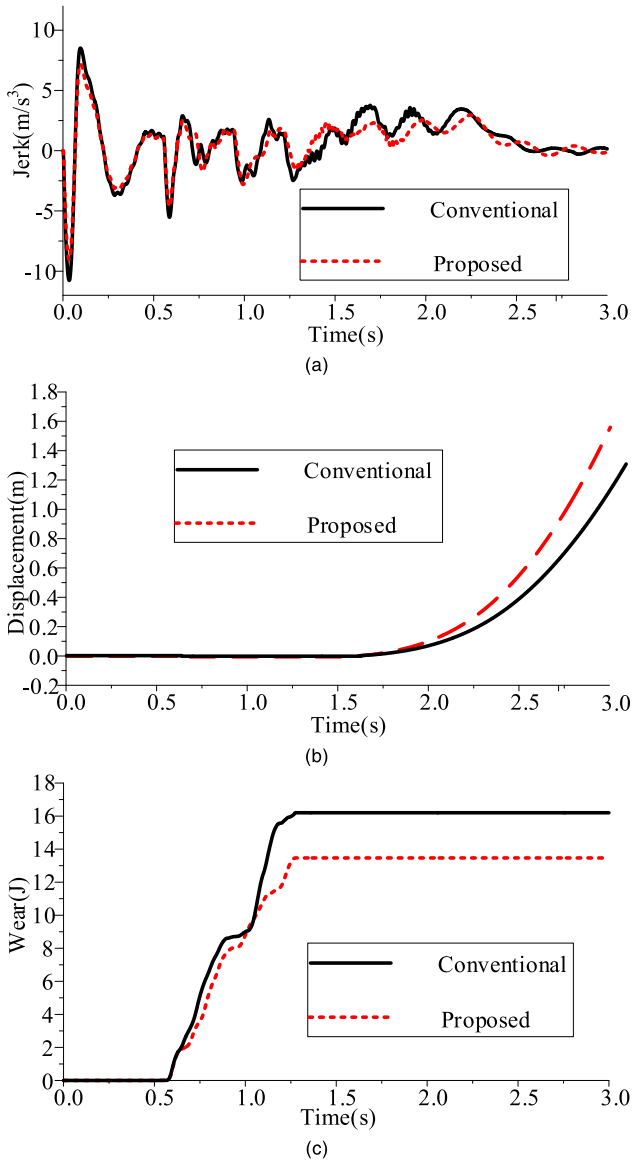

FIGURE 13. Comparison with traditional scheme. (a) Jerk, (b) Displacement, (c) Brake wear.

According to Fig. 10 and Table 3, the proposed speed estimation based on kalman filter performs well in tracking performance under different test conditions. Moreover, the maximum error is not more than 0.2 m/s, which has relatively high accuracy and timeliness, and basically meets the requirements of speed estimation.

B. THE FRONT AND REAR WHEELS ARE ON A GOOD ROAD

This section mainly describes the simulation results of the distributed driving electric vehicle under three control strategies (equal distribution of driving torque, dynamic distribution of driving torque, and dynamic distribution under torque correction). As shown in Fig. 11, the vehicle was keeping still on the slope before 0.5s. At 0.5s, the driver starts the vehicle in gear, the demand torque module starts to calculate the demand torque of the drive motor and sends the signal to each controller. The hill-start controller detects that the working conditions are met and starts to work. Then the drive motor controller starts to control each motor, and the hill-start controller starts to control the actual air pressure value to effectively track the demand air pressure. As the equal torque distribution strategy is adopted, it can be seen that the driving torque of each motor of the front and rear axles remains consistent. At 1.27s, the total driving force completely overcomes the resistance of the slope, the solenoid valve opens and inflates quickly, and the parking brake force is also quickly released. At 1.31s, the vehicle speed starts to rise slowly from 0, indicating that the hill- start controller based on the logic threshold can meet the requirements of the hill start.

TABLE 4. Comparison of evaluation indices of two control schemes.

Controller	Starting jerk(m/s³)	Rollback distance(m)	Wear(J)
Proposed	1.455	0.053	13.8
Conventional	2.388	0.176	16.9

Fig. 12 shows the simulation results of the control strategy using dynamic torque distribution strategy. As can be seen from the figure, during the uphill process, the axle load is transferred backwards, so the torque value of the drive motor of the rear axle is always greater than that of the front axle. In addition, the actual pressure of the hill-start controller also quickly follows the demand pressure, and the vehicle finally starts successfully on the ramp, indicating the effectiveness of the proposed scheme.

Fig. 13 shows the comparison results between the traditional control scheme and the control scheme proposed in this paper in three evaluation indexes. From Fig. 13(a), it can be intuitively felt that the proposed scheme has a lower jerk than the traditional scheme. Fig. 13(b) shows that neither the traditional control scheme nor the proposed control scheme has slipped, indicating that both schemes meet the safety requirements under this road condition. However, after the completion of the hill-start, it can be seen that the control scheme proposed in this paper has a faster climbing time, because the scheme based on axial load distribution can make better use of road adhesion condition. Fig. 13(c) shows that the traditional control scheme causes the brake to lose more due to the mismatch between the load of the rear axle and the motor torque. In order to quantitatively measure and evaluate the vehicle start-up jerking in the experiment, the RMS (Root Mean Square) is introduced as evaluation parameters. The equation of RMS can be expressed as:

$$RMS = \sqrt{\frac{1}{n}\sum_{k=1}^{n} j^2} \tag{25}$$

Table 4 shows the more detailed comparison results of these two schemes in terms of starting jerk, slope distance and

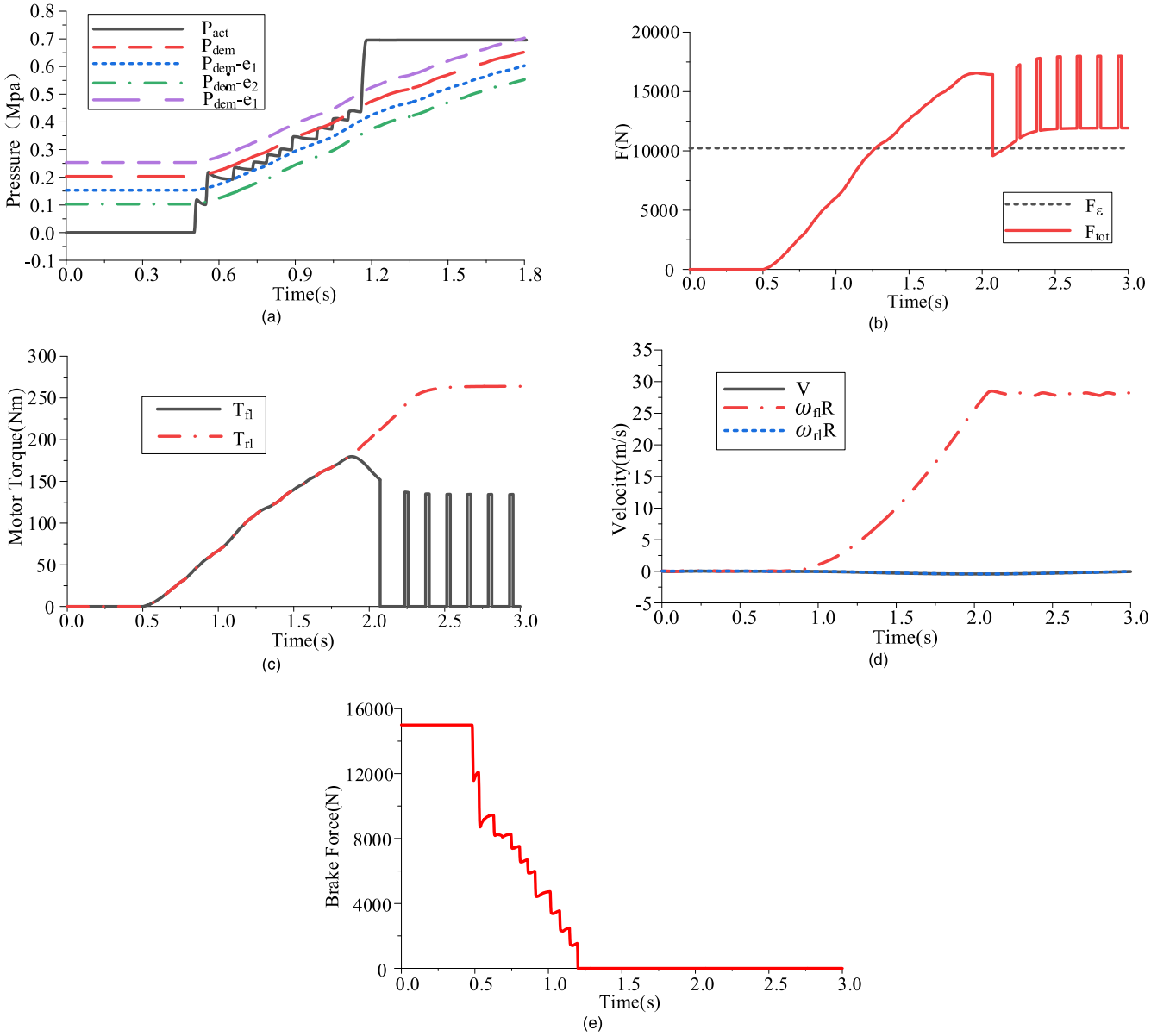

FIGURE 14. Simulation results of the equal torque distribution strategy. (a) Pressure, (b) Force, (c) Motor torque, (d) Vehicle speed and wheel speed, (e) Brake force.

brake wear. From these data, it can be seen that the proposed control scheme has better performance than the traditional control scheme.

C. THE FRONT WHEELS ARE ON BAD ADHERE CONDITION, AND THE REAR WHEELS ARE ON GOOD

As can be seen in Fig. 14, the vehicle first parked on the ramp before 0.5s. At 0.5s, the driver controls the throttle opening, and the driving motor starts to slowly increase the driving torque. At the same time, the hill-start controller starts to calculate the demand pressure and controls the actual pressure in real time through the opening and closing of the solenoid valve. At 1.28s, the driving force overcomes the ramp resistance. Then the solenoid valve quickly opens, and the parking brake force is released quickly. However, it can be seen from Fig. 14(d) that after 0.73s, the front wheel slips because the driving force exceeds the road adhesion force, and the longitudinal speed changes from 0 to a negative value, which means that the vehicle has slipped. The brake curve in the Fig. 14(e) shows that the brake force is released nearly 0.1s in advance. By 2.07s, the speed of the front wheel drive motor exceeds its maximum speed, and the driving force is rapidly reduced to 0, which has a huge impact on the safety of the vehicle.

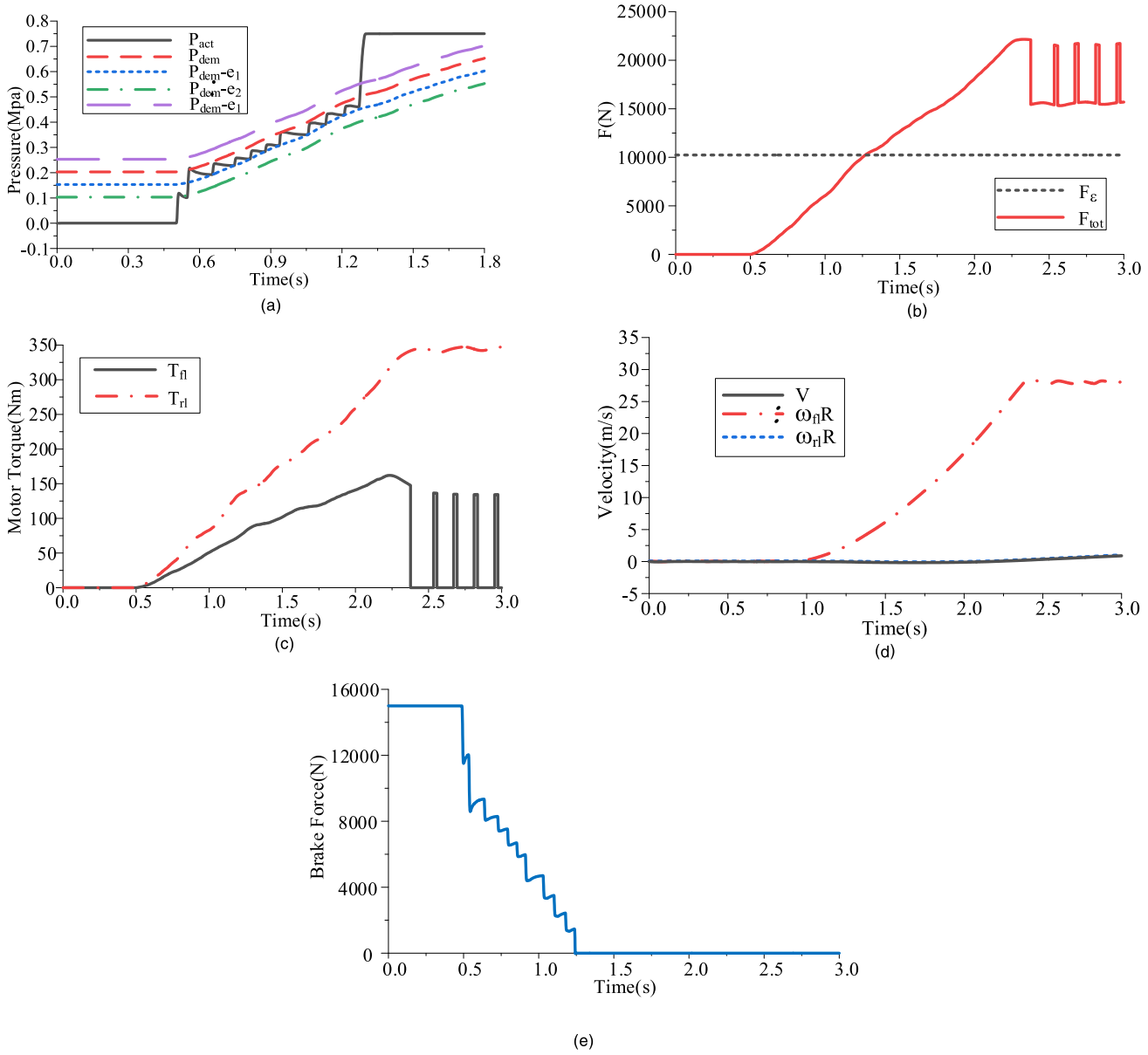

FIGURE 15. Simulation results of dynamic torque distribution strategy. (a) Pressure, (b) Force, (c) Motor torque, (d) Vehicle speed and wheel speed, (e) Brake force.

Fig. 15 shows the simulation results of dynamic distribution of driving torque. Through the distribution of driving torque, the drive motor of the rear axle outputs more torque to make better use of road adhesion force. It can be clearly seen that the hill-start controller can effectively track the demand pressure, but at 1s the front wheels still start to slip, and the vehicle speed becomes negative. As can be seen from the Fig. 15(e), the brake force is also released slightly earlier. At 2.37s, the motor speed of the front wheel also exceeds the maximum speed.

From the simulation results in Fig. 16, it can be seen that after the driving force overcomes the resistance of the slope, the hill -start controller has completed the task of releasing the parking brake force in time. Fig. 16(c) clearly shows that the torque correction controller limits the motor torques of the front axle to the maximum adhesion torque of the road and increases the torques lost by slip to the rear axle motors to maintain the total driving torque. The diagram of vehicle speed and wheel speed in Fig. 16(d) shows that the slip of the front wheels is effectively suppressed, and the effectiveness of the torque correction controller based on the sliding mode algorithm is proven.

Fig. 17 shows the comparison results of the three control schemes on the evaluation indicators. From the figure, it can

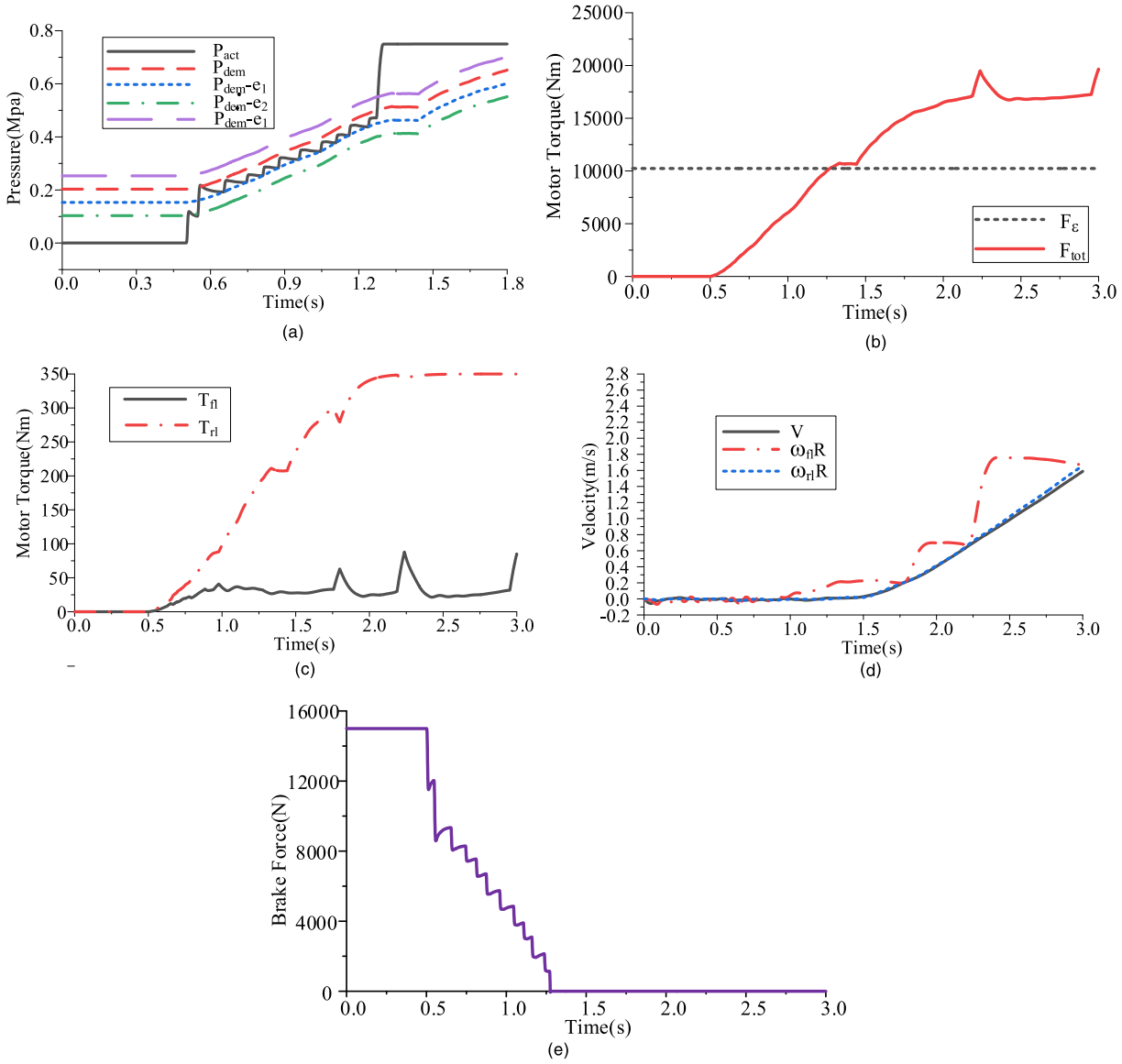

FIGURE 16. Simulation results of torque correction strategy. (a) Pressure, (b) Force, (c) Motor torque, (d) Vehicle speed and wheel speed, (e) Brake force.

TABLE 5. Comparison of evaluation indices of three control schemes.

Controller	Starting jerk(m/s^3)	Rollback distance(m)	Wear(J)
Conventional	2.165	0.52	102.2245
Proposed	2.290	0.13	64.2735
Corrected	2.321	0	47.7196

be seen that the scheme proposed in this paper has a larger jerk than the traditional scheme, which is the result of the torque correction controller. The traditional control scheme slips back 0.52m during the starting control process and keeps slipping in the following time; the second scheme without the torque correction controller no longer runs backwards after slipping 0.13m, and the third scheme with a torque correction controller does not have a backward distance. Therefore, although the proposed scheme sacrifices a little bit of starting comfort, it guarantees the safety of starting. Fig. 17(c) shows that in the traditional control scheme, the rear axle load does not match the motor torque, resulting in the vehicle's body shaking and greater brake losses. Table 5 shows the more detailed comparison results of the two schemes in terms of jerk, slope distance and brake wear. From these data, it can be seen that the proposed control scheme has better performance than the traditional control scheme.

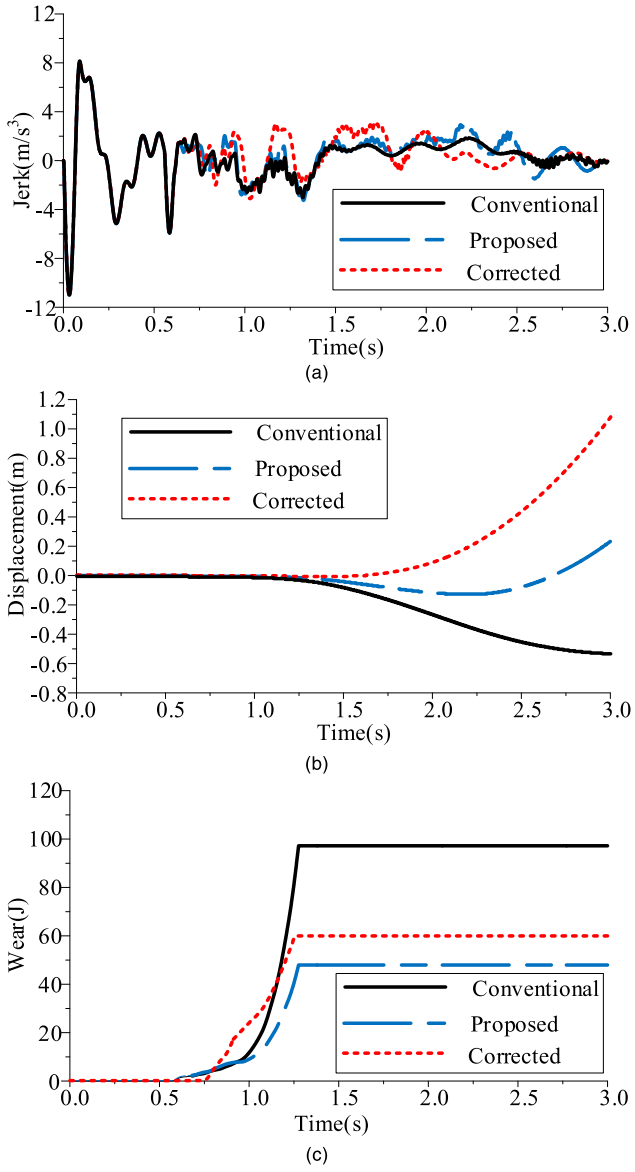

FIGURE 17. Comparison of three schemes. (a) Jerk, (b) Displacement, (c) Brake wear.

VI. CONCLUSION

In this paper, a hill-start control method suitable for the distributed drive electric vehicle is proposed to realize the vehicle to start quickly and safely on the ramp. In order to accurately estimate the speed of all-wheel-drive vehicles in real time, a vehicle speed estimation method based on Kalman filter is proposed; in order to make full use of road adhesion force, a torque control method based on front and rear axle loads is proposed; in order to deal with poor road conditions, a torque correction method based on sliding mode control is proposed. In order to accurately control the release of the parking brake force of EPB, a hill-start method based on logic threshold control is proposed. The simulation results prove the effectiveness of the proposed control strategy for the starting on the ramp, which can reduce the starting time and jerk and complete the starting task.

REFERENCES

[1] A. Nair, R. P. Sreedharan, and M. Rajesh, "Intelligent motion control of bots using hill hold assistance mechanism," in *Proc. Int. Conf. Smart Technol. For Smart Nation (SmartTechCon)*, Bangalore, India, Aug. 2017, pp. 618–621.

[2] A. Sharma, H. K. Gangwar, and D. Dabhole, "Hill start assistance developed for buses equipped with AMT," SAE Tech. Paper 2016-01-1111, 2016, doi: 10.4271/2016-01-1111.

[3] M. Paul, K. Baidya, and R. Deepak, "Electro-magnetic parking brake system for electric vehicles," SAE Tech. Paper 2019-26-0119, 2019, doi: 10.4271/2019-26-0119.

[4] I. Mohd, A. Rahim, and B. Ali, "Brake torque analysis of fully mechanical parking brake system: Theoretical and experimental approach," *Ingeniería. Investigación y Tecnología*, vol. 19, no. 1, pp. 37–49, Mar. 2018, doi: 10.22201/fi.25940732e.2018.19n1.004.

[5] X. Zhang, D. Gohlich, and J. Li, "Energy-efficient toque allocation design of traction and regenerative braking for distributed drive electric vehicles," *IEEE Trans. Veh. Technol.*, vol. 67, no. 1, pp. 285–295, Jan. 2018, doi: 10.1109/TVT.2017.2731525.

[6] L. Xiong, G. Teng, and Z. Yu, "Novel stability control strategy for distributed drive electric vehicle based on driver operation intention," *Int. J. Automot. Technol.*, vol. 17, no. 4, pp. 651–663, Aug. 2016, doi: 10.1007/s12239-016-0064-3.

[7] K. Shi, X. Yuan, and L. Liu, "Model predictive controller-based multi-model control system for longitudinal stability of distributed drive electric vehicle," *ISA Trans.*, vol. 72, pp. 44–55, Jan. 2018, doi: 10.1016/j.isatra.2017.10.013.

[8] N. Bagheri and H. Alipour, "Yaw rate control and actuator fault detection and isolation for a four wheel independent drive electric vehicle," *J. Operation Autom. Power Eng.*, vol. 5, no. 1, pp. 83–95, Jun. 2017, doi: 10.22098/joape.2017.551.

[9] S. Subramanian, "Development and testing of a control algorithm to assist drive-off in the gradient-a rapid control prototyping approach," SAE Tech. Paper 2015-26-0002, 2015, doi: 10.4271/2015-26-0002.

[10] R. Iyer, "Safety and comfort for all: An affordable hill-hold and automated parking brake system," SAE Tech. Paper 2019-26-0005, 2019, doi: 10.4271/2019-26-0005.

[11] X. Zhao, C.-Z. Liu, L. Li, Z. Zhang, S. Cheng, and X.-Y. Wang, "Cooperative control of clutch and hydraulic control unit," *IEEE Trans. Ind. Electron.*, vol. 66, no. 9, pp. 7209–7218, Sep. 2019, doi: 10.1109/TIE.2018.2874615.

[12] H. L. Wang, "Research on bang-bang control of EPB system in vehicle hill start," *Trans. Beijing Inst. Technol.*, vol. 37, no. 1, pp. 46–49, Jan. 2017, doi: 10.15918/j.tbit1001-0645.2017.01.010.

[13] P. Peng, "Research on the hill start assist of commercial vehicles based on electronic parking brake system," *Strojniski Vestnik/J. Mech. Eng.*, vol. 65, no. 1, pp. 50–60, Jan. 2019, doi: 10.5545/sv-jme.2018.5422.

[14] P. Peng, "Two-layer mass-adaptive hill start assist control method for commercial vehicles," *Proc. Inst. Mech. Eng. D, J. Automobile Eng.*, vol. 234, no. 2, pp. 438–448, Jun. 2019, doi: 10.1177/0954407019859802.

[15] E. V. Belousov, M. A. Grigor'ev, and A. A. Gryzlov, "An electric traction drive for electric vehicles," *Russian Electr. Eng.*, vol. 88, no. 4, pp. 185–188, Apr. 2017, doi: 10.3103/S1068371217040034.

[16] N. K. Saxena, S. Gebrehiwot, and D. Mena, "Controller design for electric motor derived vehicle," *Indonesian J. Electr. Eng. Informat.*, vol. 6, no. 2, pp. 125–131, Jun. 2018, doi: 10.11591/ijeei.v6i2.282.

[17] M. Song, "Design and research of intelligent vehicle EPB controller based on ISO26262 standard," SAE Tech. Paper 2019-01-5049, 2019, doi: 10.4271/2019-26-0005.

[18] Q. Zhang, H. Wang, and W. Gu, "Design and research of pneumatic control solenoid valve of hill start assist system of the medium and heavy duty vehicles," *Chin. Hydraul. Pneum.*, vol. 11, pp. 15–19, Nov. 2016, doi: 10.11832/j.issn.1000-4858.2016.11.003.

[19] Y. Chen, S. Chen, Y. Zhao, Z. Gao, and C. Li, "Optimized handling stability control strategy for a four in-wheel motor independent-drive electric vehicle," *IEEE Access*, vol. 7, pp. 17017–17032, 2019, doi: 10.1109/ACCESS.2019.2893894.

[20] C. Zhang, D. Zhang, H. Zeng, R. Wang, J. Wen, and W. Mo, "Research of smoothness on torque coordination of two-wheel independently driven hub electric vehicle based on fuzzy control," *Noise Vibrat. Worldwide*, vol. 50, no. 7, pp. 205–216, Jul. 2019, doi: 10.1177/0957456519860841.

[21] B. Peng, H. Zhang, and P. Zhao, "Research on the stability control strategy of four-wheel independent driving electric vehicle," *Engineering*, vol. 9, no. 3, pp. 338–350, Mar. 2017, doi: 10.4236/eng.2017.93018.

[22] H. Chu, "Application of slope sensor in hill-start to AMT (automated manual transmission) vehicles," SAE Tech. Paper 2015-01-1108, 2015, doi: 10.4271/2015-01-1108.
[23] J. Huang, Y. Liu, M. Liu, M. Cao, and Q. Yan, "Multi-objective optimization control of distributed electric drive vehicles based on optimal torque distribution," *IEEE Access*, vol. 7, pp. 16377–16394, 2019, doi: 10.1109/ACCESS.2019.2894259.
[24] Y. A. Khan and V. Verma, "Novel speed estimation technique for vector-controlled switched reluctance motor drive," *IET Electric Power Appl.*, vol. 13, no. 8, pp. 1193–1203, Aug. 2019, doi: 10.1049/iet-epa.2018.5572.

LEI WU received the B.E. degree from the Nanjing Institute of Technology, Nanjing, China, in 2018. He is currently pursuing the M.S. degree in vehicle engineering with the Nanjing University of Science and Technology, Nanjing. His research interests include vehicle dynamic simulation, intelligent control for electric vehicle, and automatic driving control.

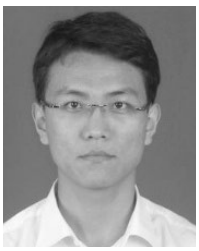

HONGLIANG WANG received the B.E. and Ph.D. degrees in vehicle engineering from the Beijing Institute of Technology, Beijing, China, in 2005 and 2010, respectively.

He was a Visiting Scholar with the University of Waterloo, in 2017. He is currently an Assistant Professor with the School of Mechanical Engineering, Nanjing University of Science and Technology, Nanjing, China. His research interests include vehicle system dynamics, intelligent wire control technology of vehicle chassis, and automatic transmission.

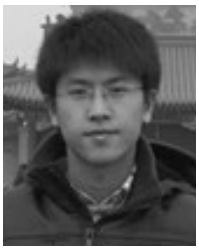

DAWEI PI received the B.E. and Ph.D. degrees in vehicle engineering from Southeast University, Nanjing, China, in 2005 and 2010, respectively.

He was a Visiting Scholar with The Ohio State University, in 2017. He is currently an Assistant Professor with the School of Mechanical Engineering, Nanjing University of Science and Technology, Nanjing. His research interests include vehicle system dynamics, intelligent control for electric vehicles, and intelligent fault-tolerant control of electro-mechanical systems.

ERLIE WANG received the B.E. degree in vehicular engineering from Chang'an University, Xi'an, China, in 2009, and the Ph.D. degree in vehicular engineering from the Beijing Institute of Technology, Beijing, China, in 2015.

He is currently a Lecturer with the School of Mechanical Engineering, Nanjing University of Science and Technology, Nanjing, China. His research interests include vehicle system dynamics, intelligent wire control technology of vehicle chassis, and automatic transmissions.

XIA WANG received the M.S. degree in vehicular engineering from the Nanjing University of Science and Technology, Nanjing, China. She is currently a Lecturer with the School of Mechanical Engineering, Nanjing University of Science and Technology. Her research interests include vehicle dynamic simulation, intelligent control for electric vehicles, and automatic driving control.